Journal of Alloys and Compounds 509 (2011) 7277–7282

Contents lists available at ScienceDirect

Journal of Alloys and Compounds

journal homepage: www.elsevier.com/locate/jallcom

Combustion synthesis of $Ti_3Si_{1-x}Al_xC_2$ solid solutions from TiC-, SiC-, and Al_4C_3-containing powder compacts

C.L. Yeh*, J.H. Chen

Department of Aerospace and Systems Engineering, Feng Chia University, 100 Wenhwa Road, Seatwen, Taichung 40724, Taiwan

ARTICLE INFO

Article history:
Received 1 April 2011
Received in revised form 10 April 2011
Accepted 11 April 2011
Available online 21 April 2011

Keywords:
Ceramics
X-ray diffraction
SEM
$Ti_3Si_{1-x}Al_xC_2$
Combustion synthesis

ABSTRACT

Preparation of the $Ti_3Si_{1-x}Al_xC_2$ solid solution with $x = 0.2–0.8$ was investigated by self-propagating high-temperature synthesis (SHS) using TiC-, SiC-, and Al_4C_3-containing powder compacts. Due to the variation of reaction exothermicity with sample stoichiometry, the combustion temperature and reaction front velocity decreased with increasing Al content of $Ti_3Si_{1-x}Al_xC_2$ for the TiC- and Al_4C_3-added samples, but increased for the samples with SiC. In contrast to the formation of $Ti_3(Si,Al)C_2$ as the dominant phase for the TiC- and SiC-added samples, TiC was identified as the major constituent in the final products of samples adopting Al_4C_3. In addition, the evolution of $Ti_3(Si,Al)C_2$ was improved by increasing the Al content of the TiC- and SiC-added powder compacts, but deteriorated considerably upon the increase of Al_4C_3 in the Al_4C_3-containing sample.

1. Introduction

Layered ternary compounds $M_{n+1}AX_n$, where $n = 1$, 2, or 3, M is an early transition metal, A is an A-group (mostly IIIA and IVA) element, and X is either C or N, are a new class of materials with properties featuring many merits of metals and ceramics [1–3]. In general, they are relatively soft, readily machinable, good thermal and electrical conductors, elastically stiff, and highly resistant to thermal shock, oxidation, and corrosion [1–6]. The representative MAX phases, such as Ti_3SiC_2, Ti_3AlC_2, Ti_2AlC, Cr_2AlC, and Ti_2AlN, have been extensively studied [4–13]. Comprehensive reviews are given in Refs. [11,12], which present microstructural characterizations, formation mechanisms, and material properties of the MAX ceramics. Moreover, there are a variety of fabrication routes for the MAX compounds, including hot pressing (HP) [2,4,5], hot isostatic pressing (HIP) [6,7], pulse discharge sintering (PDS) [14–16], in situ hot pressing/solid–liquid reaction synthesis [17–20], infiltration method [21], self-propagating high-temperature synthesis (SHS) [22–28], etc.

The solid solution based on the MAX phases can be formed by substitution on the M, A, or X site, which renders great potential for tailoring and/or optimizing the material properties. Many MAX-based solid solutions, such as $(Ti,Nb)_2AlC$, $(Cr,V)_2AlC$, $Ti_3(Si,Al)C_2$, and $Ti_2Al(C,N)$, were successfully produced and their mechanical and thermal properties were explored [29–38]. Of particular interest for this work are $Ti_3Si_{1-x}Al_xC_2$ solid solutions which possess enhanced properties when compared with their related end members Ti_3SiC_2 and Ti_3AlC_2 [31–34]. By means of the in situ hot pressing/solid–liquid reaction synthesis at 1500 °C for 60 min, $Ti_3Si_{1-x}Al_xC_2$ solid solutions with a wide stoichiometric range were produced from elemental powders [31,32]. As reported by Zhang et al. [32], the samples composed of additional Si and a reduced amount of graphite facilitated the formation of $Ti_3Si_{1-x}Al_xC_2$ with high Al contents. The $Ti_3Si_{0.5}Al_{0.5}C_2$ sample was also fabricated from the mixture of Ti, SiC, Al, and C powders by HIP at 1400 °C and 100 MPa for 10 h [35].

With the advantages of time and energy savings, combustion synthesis particularly in the mode of self-propagating high-temperature synthesis (SHS) represents an attractive method of producing advanced materials including borides, carbides, nitrides, silicides, carbonitrides, intermetallics, etc. [39–41]. The SHS reaction of the solid state has been utilized to prepare a number of MAX carbides, like Ti_3SiC_2 [22,23], Ti_3AlC_2 [24,25], Nb_2AlC [26], Cr_2AlC [27], and Ti_2SnC [28]. According to Yeh and Shen [22,23], the addition of a proper amount of TiC or SiC to the elemental powder compacts was beneficial for the production of Ti_3SiC_2 by combustion synthesis. The evolution of Ti_3AlC_2 was also substantially enhanced by adopting TiC- and Al_4C_3-containing samples [24,25]. Recently, the SHS reaction involving gaseous reagents was performed to fabricate the $Ti_2AlC_{0.5}N_{0.5}$ solid solution from TiC-, TiN-, and Al_4C_3-diluted samples in nitrogen [36,37].

As the first attempt, this study aims to prepare $Ti_3Si_{1-x}Al_xC_2$ solid solutions with a broad stoichiometric range by the SHS process from TiC-, SiC-, and Al_4C_3-containing samples. The effect of

* Corresponding author. Tel.: +886 4 24517250x3963; fax: +886 4 24510862.
E-mail address: clyeh@fcu.edu.tw (C.L. Yeh).

0925-8388/$ – see front matter © 2011 Elsevier B.V. All rights reserved.
doi:10.1016/j.jallcom.2011.04.076

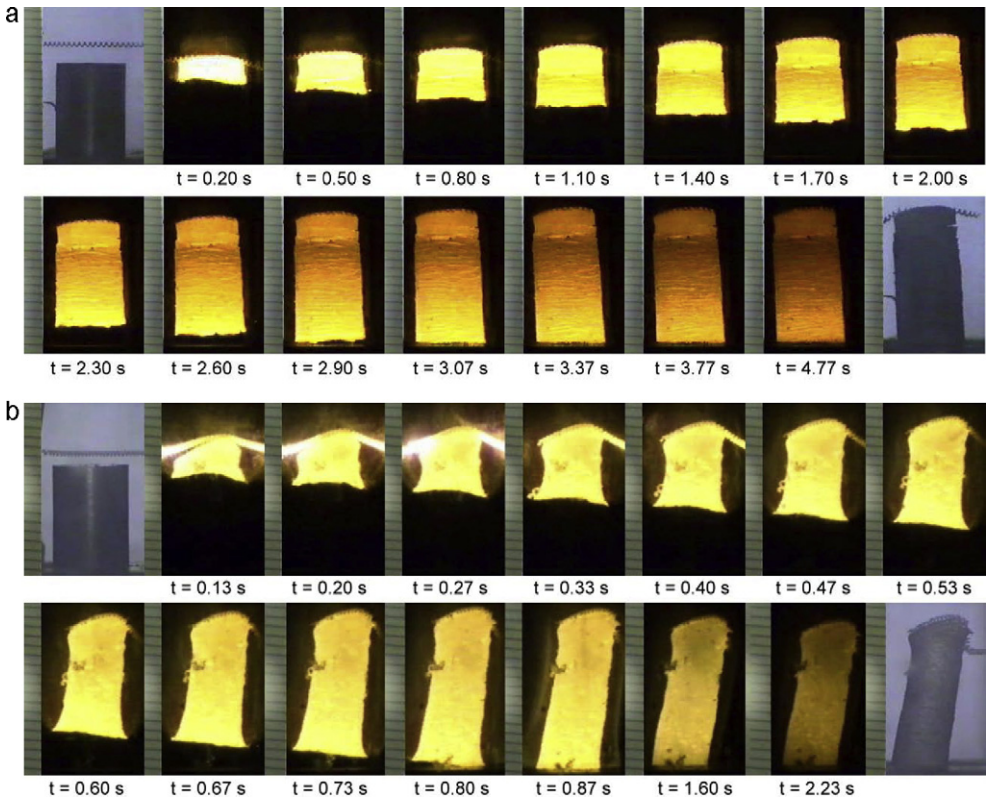

Fig. 1. Recorded images illustrating propagation of self-sustaining combustion along (a) a TiC-containing sample with $x = 0.4$, and (b) a SiC-containing sample with $x = 0.8$.

initial sample composition is investigated on the phase constituents and morphology of the final product, as well as on the combustion behavior such as combustion temperature and propagation velocity of the reaction front.

2. Experimental methods of approach

Titanium (Strem Chemicals, ≤45 μm, 99%), aluminum (Showa Chemical Co., ≤40 μm, 99%), silicon (Strem Chemicals, ≤45 μm, 99.5%), and carbon black (Showa Chemical Co.) powders are used as the elemental components in this study. In addition, three metal carbides, TiC (Aldrich Chemical, ≤45 μm, 98%), SiC (Aldrich Chemical, ≤40 μm, 99%), and Al_4C_3 (Strem Chemicals, ≤45 μm, 98%), are adopted as the starting reagents. The initial reactant compositions according to the samples containing TiC, SiC, and Al_4C_3 are formulated as Reactions (1), (2), and (3), respectively.

$$2Ti + (1-x)Si + xAl + C + TiC \rightarrow Ti_3Si_{1-x}Al_xC_2 \quad (1)$$

$$3Ti + (1-x)SiC + xAl + (1+x)C \rightarrow Ti_3Si_{1-x}Al_xC_2 \quad (2)$$

$$3Ti + (1-x)Si + (2-0.75x)C + 0.25xAl_4C_3 \rightarrow Ti_3Si_{1-x}Al_xC_2 \quad (3)$$

where the stoichiometric parameter x represents the Al content of $Ti_3Si_{1-x}Al_xC_2$. It should be noted that there are no elemental Si and Al powders included in the SiC- and Al_4C_3-added samples, respectively. Reactant powders based upon Reactions (1)–(3) were prepared with x varying from 0.2 to 0.8 and then mixed in a ball mill. The initial compositions of test samples conducted in this study are summarized in Table 1. Powder mixtures were cold-pressed into the cylindrical compact with a diameter of 7 mm, a height of 12 mm, and a compaction density of 60% relative to the theoretical maximum density (TMD). The SHS experiment was performed in a stainless-steel windowed chamber under an atmosphere of high purity argon (99.99%). Details of the experimental setup and measurement approach were reported elsewhere [42].

Table 1
Summary of initial compositions of test samples conducted in this study.

Type of sample	Sample stoichiometry	Parameter, x
TiC-containing	$2Ti + (1-x)Si + xAl + C + TiC$	0.2, 0.4, 0.6, 0.8
SiC-containing	$3Ti + (1-x)SiC + xAl + (1+x)C$	0.2, 0.4, 0.6, 0.8
Al_4C_3-containing	$3Ti + (1-x)Si + (2-0.75x)C + 0.25xAl_4C_3$	0.2, 0.4, 0.6, 0.8

3. Results and discussion

3.1. Observation of combustion characteristics

Fig. 1(a) and (b) presents two recorded SHS sequences illustrating different propagation modes of the combustion wave typically observed in this study. For the TiC-added sample with $x = 0.4$, Fig. 1(a) indicates that the combustion front forms several localized reaction zones moving along a spiral trajectory. The spinning combustion wave left visible tracks on the sample surface. On the other hand, as shown in Fig. 1(b), the SHS process of the powder compact adopting SiC under $x = 0.8$ is characterized by a nearly planar combustion front traversing the sample longitudinally at a much faster rate than that of Fig. 1(a). This implies lower exothermicity for the SHS reaction associated with Fig. 1(a). It is believed that for the reactant compacts conducted by this study, the thermal energy released by the reaction of Ti with carbon plays an important role in sustaining the combustion wave. Because of different metal carbides involved in the reactant mixtures, Reaction (1) produces a lesser amount of TiC from the reaction of Ti with carbon when compared to Reactions (2) and (3). This might be responsible for the spinning combustion wave observed for the TiC-containing sample, while the planar reaction front with a high propagation rate for the SiC- and Al_4C_3-added samples. However, it should be noted that self-sustaining combustion of the Al_4C_3-added powder compact with $x = 0.8$ no longer features a planar front, due most likely to the reduced reaction exothermicity on account of the increase of Al_4C_3 in the reactant mixture.

Furthermore, as illustrated in Fig. 1(a) and (b), the burned samples were subjected to axial elongation and radial contraction after the passage of the combustion wave. Formation of the elongated and slightly slender products has been reported in the combustion synthesis of many MAX carbides, including Ti_3SiC_2 [22,23], Ti_3AlC_2 [24,25] and Ti_2SnC [28]. According to the previous studies [22–25],

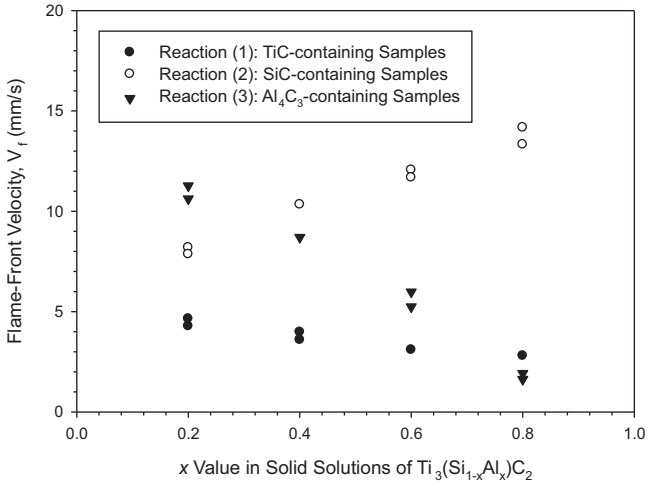

Fig. 2. Variations of flame-front propagation velocity with Al content of $Ti_3Si_{1-x}Al_xC_2$ solid solutions synthesized from samples containing different types of metal carbides.

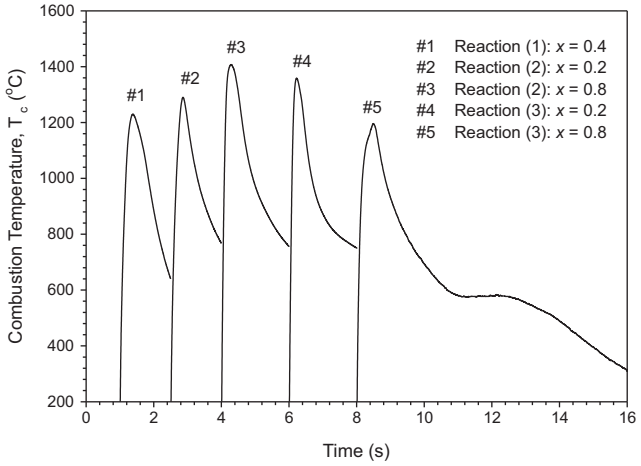

Fig. 3. Dependence of combustion temperature on Al content of $Ti_3Si_{1-x}Al_xC_2$ solid solutions synthesized from samples of different stoichiometries.

the axial elongation of the burned sample is mainly attributed to the growth of MAX grains into a terraced structure. The radial contraction is a consequence of the surface tension effect of the liquid melt formed in the reaction sequence. The liquid phase substances taken into account in the combustion systems of Reactions (1)–(3) could include molten Al and intermetallic compounds such as Ti_3Al, TiAl, and Ti_5Si_3.

3.2. Measurement of flame-front propagation velocity and combustion temperature

Fig. 2 presents the composition dependence of the flame-front propagation velocity (V_f) for the samples involving different metal carbides. As shown in Fig. 2, the reaction front velocity of the TiC-added sample decreases from 4.7 to 2.8 mm/s upon the production of $Ti_3Si_{1-x}Al_xC_2$ solid solutions with increasing Al content from $x = 0.2$ to 0.8. The increase of Al means a corresponding decrease in Si for the reactant mixture of Reaction (1), which reduces the overall reaction exothermicity due to less heat released from the reaction of Ti with Al than that of Ti with Si [43]. Consequently, the reaction front is decelerated. Moreover, the flame-front velocity of the TiC-added sample is lower than those of the samples adopting SiC and Al_4C_3. As mentioned above, this could be attributed to the weaker exothermic nature of Reaction (1) in comparison to Reactions (2) and (3).

For the powder compacts of Reaction (2), Fig. 2 indicates that the increase of Al leads to a significant increase in the combustion velocity from 7.9 to 14.2 mm/s. According to Reaction (2), the increase of Al in the SiC-containing sample is accompanied by a decrease in SiC and an increase in carbon. Since SiC contributes a dilution effect to combustion but carbon reacts exothermically with Ti, the overall reaction exothermicity is augmented when $Ti_3Si_{1-x}Al_xC_2$ with a higher content of Al is synthesized. On the contrary, the flame-front velocity of the Al_4C_3-containing sample decreases substantially from 11.3 to 1.9 mm/s with increasing Al_4C_3 for the formation of $Ti_3Si_{1-x}Al_xC_2$ with a higher proportion of Al. This is because partly of a decrease in carbon to compensate for the increase of Al_4C_3. In part, for a sample containing more Al_4C_3 the energy dissipated to thermally decompose Al_4C_3 is increased. As a result, the reaction exothermicity is diminished and the reaction rate is retarded.

Fig. 3 plots measured temperature profiles from solid state combustion of the TiC-, SiC, and Al_4C_3-containing samples. As shown in Fig. 3, the abrupt rise in temperature signifies the rapid arrival of the combustion wave and the peak value corresponds to the combustion front temperature. After the passage of the reaction front, an appreciable decrease in temperature is a consequence of the heat loss to the surroundings. The reaction front temperature of about 1230 °C measured from the sample of Reaction (1) with $x = 0.4$ is indicated in Fig. 3. For the TiC-containing samples, the experimental results of this study showed the combustion front temperature ranging between 1210 and 1270 °C.

Fig. 3 also reveals that the peak reaction temperature of the SiC-added sample increases from 1290 to 1407 °C as the stoichiometric parameter x in Reaction (2) rises from 0.2 to 0.8, confirming the increase of reaction exothermicity with Al content of the $Ti_3Si_{1-x}Al_xC_2$ solid solution formed from the SiC-added sample. However, the combustion temperature of the Al_4C_3-containing sample is decreased from 1360 to 1196 °C by increasing the parameter x in Reaction (3). This suggests the decrease of reaction exothermicity with increasing Al_4C_3 in the sample. It is very important to note that for the samples of three types the composition dependence of the combustion temperature is in a manner consistent with that of reaction front velocity.

3.3. Composition and morphology analysis of combustion products

Fig. 4(a) and (b) depicts the XRD patterns of as-synthesized $Ti_3Si_{1-x}Al_xC_2$ solid solutions from the TiC-added samples with a low ($x = 0.2$) and high ($x = 0.8$) Al content, respectively. In addition to the formation of $Ti_3(Si,Al)C_2$ as the dominant phase, Fig. 4(a) indentifies the presence of two minor compounds TiC and SiC. The binary carbide TiC has been considered as a key intermediate in the synthesis of Ti_3SiC_2 and Ti_3AlC_2 [22,24]. An improvement in the evolution of $Ti_3(Si,Al)C_2$ is shown in Fig. 4(b), which is substantiated by a lesser amount of TiC and no detection of SiC in the final product.

According to Fig. 5(a), the SiC-added sample with $x = 0.2$ produces $Ti_3(Si,Al)C_2$ along with three minor phases, TiC, SiC, and Ti_3Al. Similar to that observed for the sample initially comprising TiC, a better degree of $Ti_3(Si,Al)C_2$ formation was achieved by increasing Al in the reactant mixture. As revealed in Fig. 5(b) the intermetallic phase Ti_3Al no longer exists and binary carbides TiC and SiC are reduced in the $Ti_3(Si,Al)C_2$ solid solution synthesized from the SiC-added sample with $x = 0.8$.

For the Al_4C_3-containing samples with $x = 0.2$ and 0.8, the XRD patterns of final products are presented in Fig. 6(a) and (b), respectively. In spite of the production of $Ti_3(Si,Al)C_2$, Fig. 6(a) points out a

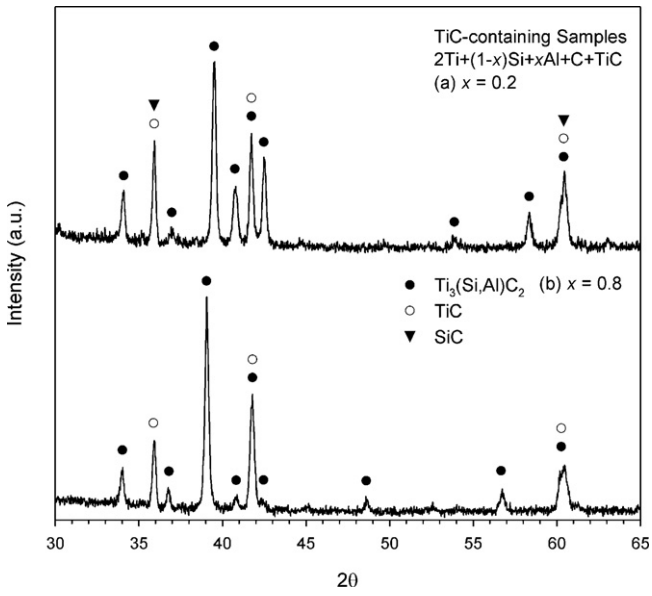

Fig. 4. XRD patterns of synthesized products from TiC-containing samples with (a) $x = 0.2$ and (b) $x = 0.8$.

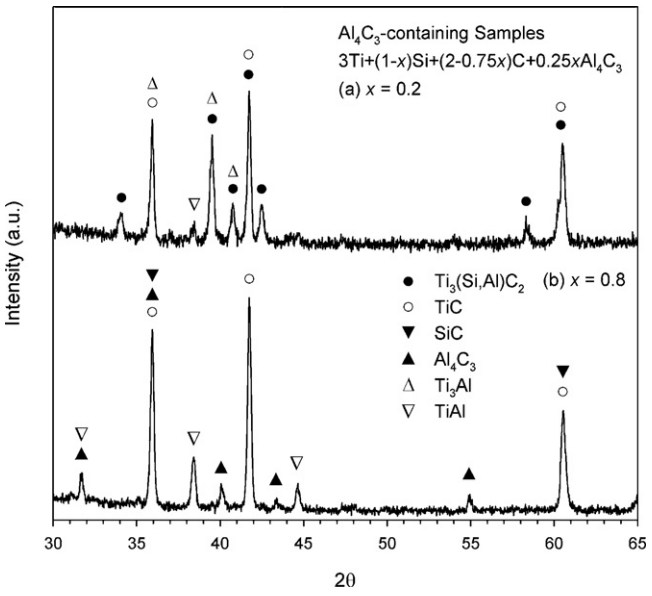

Fig. 6. XRD patterns of synthesized products from Al_4C_3-containing samples with (a) $x = 0.2$ and (b) $x = 0.8$.

large amount of TiC and several minor phases including SiC, Ti_3Al, and TiAl. The intermetallic compounds, Ti_3Al and TiAl, could be yielded through the reaction of Ti with Al_4C_3. As the content of Al_4C_3 increases in the green sample up to $x = 0.8$, Fig. 6(b) indicates the absence of $Ti_3(Si,Al)C_2$ in the resulting product which is composed of TiC, SiC, TiAl, and Al_4C_3 with TiC as the dominant phase. This implies that the use of Al_4C_3 as a reactant is unfavorable for the formation of $Ti_3(Si,Al)C_2$ solid solutions with high contents of Al.

Table 2 summarizes the dominant and secondary phases of the final products with respect to TiC-, SiC-, and Al_4C_3-containing samples of different initial stoichiometries. Among three different types of the samples, the optimum yield of $Ti_3(Si,Al)C_2$ solid solutions was achieved by the TiC-added sample. This suggests that the TiC-added sample provides not only the most favorable reactant composition, but also the most appropriate reaction temperature and time for the formation of $Ti_3(Si,Al)C_2$, because it was found by previous studies [22,24,28] that the high combustion temperature and short reaction time associated with the SHS process are adverse for the production of ternary carbides. Additionally, an improved phase evolution was obtained in $Ti_3(Si,Al)C_2$ with a higher content of Al for TiC- and SiC-containing samples, but the opposite was observed for the Al_4C_3-added sample.

Typical microstructures of the synthesized products dominated by the $Ti_3(Si,Al)C_2$ solid solution are presented in Fig. 7(a) and (b), which are related with TiC- and SiC-containing powder compacts, respectively. Fig. 7(a) and (b) shows that plate-like $Ti_3(Si,Al)C_2$ grains are closely stacked into a laminated structure characteristic of the ternary MAX carbide. On the other hand, Fig. 7(c) displays a different microstructure featuring granular grains of TiC produced from the Al_4C_3-added sample of $x = 0.8$.

Vickers hardness of the $Ti_3(Si,Al)C_2$ solid solutions synthesized from TiC- and SiC-added samples is between 6.2 and 6.8 GPa, which increases with decreasing Al content of $Ti_3(Si,Al)C_2$. Due to the presence of TiC as a secondary phase in the final product, Vickers hardness of the as-synthesized $Ti_3(Si,Al)C_2$ solid solution is higher than 3.5 and 4.0 GPa for Ti_3AlC_2 and Ti_3SiC_2, respectively. The fracture toughness and compressive strength of $Ti_3(Si,Al)C_2$ are about 6.6 $MPa{\cdot}m^{1/2}$ and 810 MPa, both of which are within those of Ti_3AlC_2 and Ti_3SiC_2. This suggests that the mechanical properties of $Ti_3(Si,Al)C_2$ can be tailored by adjusting the relative proportion between Si and Al.

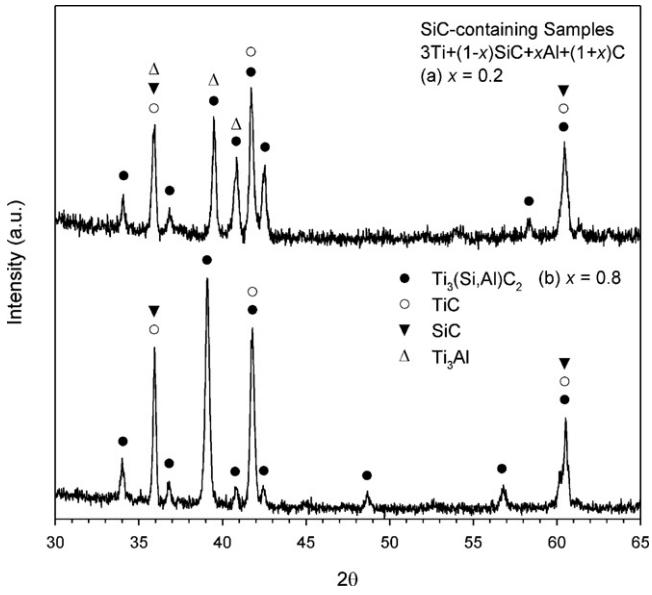

Fig. 5. XRD patterns of synthesized products from SiC-containing samples with (a) $x = 0.2$ and (b) $x = 0.8$.

Table 2
Summary of phase constituents of synthesized products with respect to their initial sample stoichiometry.

Sample stoichiometry		Phase constituents of SHS products		
Reaction	Parameter, x	Dominantphase	Secondary phases	
			Carbides	Intermetallics
(1)	0.2, 0.4	$Ti_3(Si,Al)C_2$	TiC, SiC	
(1)	0.6, 0.8	$Ti_3(Si,Al)C_2$	TiC	
(2)	0.2, 0.4	$Ti_3(Si,Al)C_2$	TiC, SiC	Ti_3Al
(2)	0.6, 0.8	$Ti_3(Si,Al)C_2$	TiC, SiC	
(3)	0.2	TiC	$Ti_3(Si,Al)C_2$	Ti_3Al, TiAl
(3)	0.4, 0.6	TiC	$Ti_3(Si,Al)C_2$	TiAl
(3)	0.8	TiC	SiC, Al_4C_3	TiAl

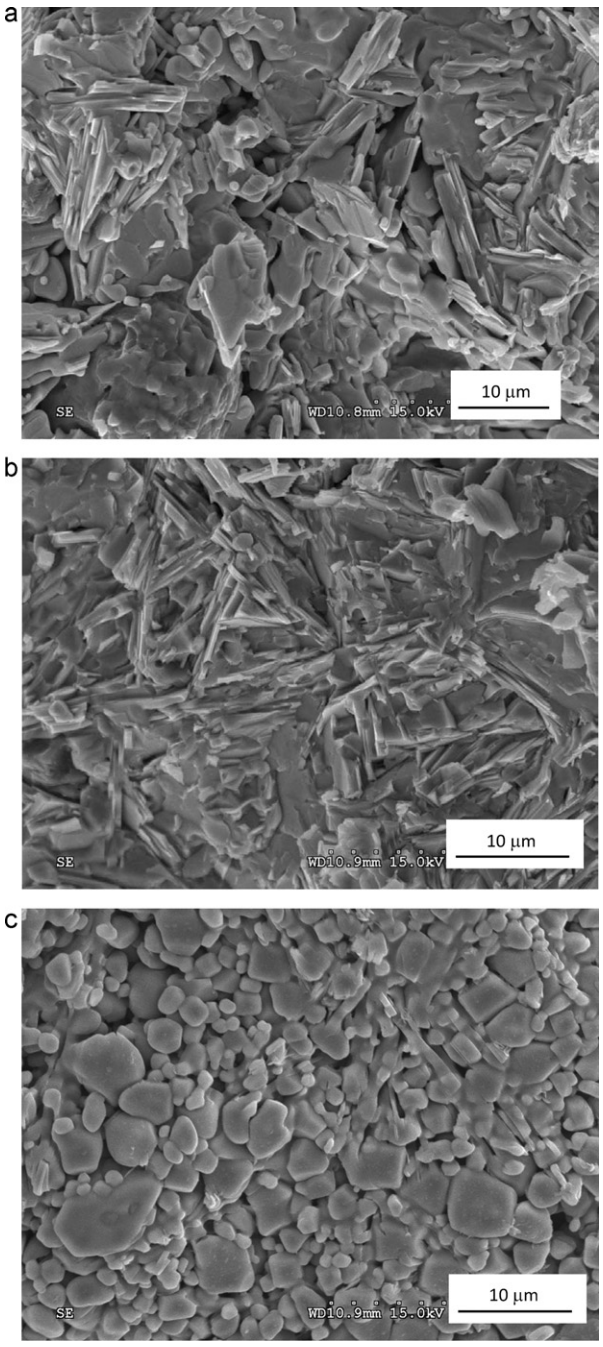

Fig. 7. SEM micrographs illustrating fracture surfaces of products synthesized from (a) TiC-, (b) SiC-, and (c) Al_4C_3-containing samples with $x = 0.8$.

4. Conclusions

Preparation of the $Ti_3Si_{1-x}Al_xC_2$ solid solutions with $x = 0.2$–0.8 was conducted by the SHS process using TiC-, SiC-, and Al_4C_3-containing powder compacts. On account of the variation of reaction exothermicity with sample stoichiometry, it was found that with an increase in the Al content of as-synthesized $Ti_3Si_{1-x}Al_xC_2$ the combustion temperature and reaction front velocity decreased moderately for the TiC-added sample but substantially for the sample adopting Al_4C_3. However, a significant increase in both combustion wave temperature and velocity was observed for the SiC-added sample. In terms of combustion, the TiC-containing powder compact is the least exothermic of the three samples with different metal carbides. The fastest reaction front with a speed of 14.2 mm/s and a temperature of 1407 °C was detected in the synthesis of $Ti_3Si_{1-x}Al_xC_2$ with $x = 0.8$ from the SiC-added sample.

For the TiC- and SiC-containing powder compacts, the $Ti_3(Si,Al)C_2$ solid solution was identified as the dominant phase in their final products and $Ti_3(Si,Al)C_2$ with a higher content of Al was more preferably yielded. Based upon the XRD patterns, the final products contain TiC as a second phase and some other minor species like SiC and Ti_3Al. For the Al_4C_3-added samples, however, the resulting products are dominated by TiC. Additionally, the formation of $Ti_3(Si,Al)C_2$ was considerably deteriorated by increasing Al_4C_3 in the reactant mixture. According to the experimental evidence of this study, among the samples of three different types the TiC-containing sample is the most favorable for the preparation of $Ti_3(Si,Al)C_2$ through the SHS process.

Acknowledgement

This research was sponsored by the National Science Council of Taiwan, ROC, under the grant of NSC 98-2221-E-035-065-MY2.

References

[1] M.W. Barsoum, The $M_{N+1}AX_N$ phases: a new class of solids; thermodynamically stable nanolaminates, Prog. Solid State Chem. 28 (2000) 201–281.
[2] M.W. Barsoum, D. Brodkin, T. El-Raghy, Layered machinable ceramics for high temperature applications, Scripta Mater. 36 (5) (1997) 535–541.
[3] P. Eklund, M. Beckers, U. Jansson, H. Högberg, L. Hultman, The $M_{n+1}AX_n$ phases: materials science and thin-film processing, Thin Solid Films 518 (2010) 1851–1878.
[4] M.W. Barsoum, T. El-Raghy, Synthesis and characterization of a remarkable ceramic: Ti_3SiC_2, J. Am. Ceram. Soc. 79 (7) (1996) 1953–1956.
[5] W.B. Tian, P.L. Wang, G.J. Zhang, Y.M. Kan, Y.X. Li, D.S. Yan, Synthesis and thermal and electrical properties of bulk Cr_2AlC, Scripta Mater. 54 (2006) 841–846.
[6] N.V. Tzenov, M.W. Barsoum, Synthesis and characterization of Ti_3AlC_2, J. Am. Ceram. Soc. 83 (4) (2000) 825–832.
[7] M.W. Barsoum, M. Ali, T. El-Raghy, Processing and characterization of Ti_2AlC, Ti_2AlN, and $Ti_2AlC_{0.5}N_{0.5}$, Metall. Mater. Trans. 31A (2000) 1857–1865.
[8] J.Y. Wang, Y.C. Zhou, Recent progress in theoretical prediction, preparation, and characterization of layered ternary transition-metal carbides, Annu. Rev. Mater. Res. 39 (2009) 415–443.
[9] Z.J. Lin, M.S. Li, J.Y. Wang, Y.C. Zhou, High-temperature oxidation and hot corrosion of Cr_2AlC, Acta Mater. 55 (2007) 6182–6191.
[10] Z.J. Lin, M.J. Zhuo, Y.C. Zhou, M.S. Li, J.Y. Wang, Microstructural characterization of layered ternary Ti_2AlC, Acta Mater. 54 (2006) 1009–1015.
[11] H.B. Zhang, Y.W. Bao, Y.C. Zhou, Current status in layered ternary carbide Ti_3SiC_2, a review, J. Mater. Sci. Technol. 25 (2009) 1–38.
[12] Z.J. Lin, M.S. Li, Y.C. Zhou, TEM investigations on layered ternary ceramics, J. Mater. Sci. Technol. 23 (2007) 145–165.
[13] C.L. Yeh, C.W. Kuo, F.S. Wu, Formation of Ti_2AlN by solid-gas combustion synthesis with AlN- and TiN-diluted samples in nitrogen, Int. J. Appl. Ceram. Technol. 7 (2010) 730–737.
[14] W.B. Tian, Z.M. Sun, H. Hashimoto, Y.L. Du, Microstructure evolution and mechanical properties of Ti_3SiC_2-TiC composites, J. Alloys Compd. 502 (2010) 49–53.
[15] Y. Zou, Z.M. Sun, H. Hashimoto, L. Cheng, Synthesis reactions for Ti_3AlC_2 through pulse discharge sintering TiH_2/Al/C powder mixture, J. Alloys Compd. 468 (2009) 217–221.
[16] W.B. Tian, Z.M. Sun, Y.L. Du, H. Hashimoto, Mechanical properties of pulse discharge sintered Cr_2AlC at 25–1000 °C, Mater. Lett. 63 (2009) 670–672.
[17] X.H. Wang, Y.C. Zhou, Microstructure and properties of Ti_3AlC_2 prepared by the solid–liquid reaction synthesis and simultaneous in-situ hot pressing process, Acta Mater. 50 (2002) 3141–3149.
[18] Z.J. Lin, Y.C. Zhou, M.S. Li, J.Y. Wang, In-situ hot pressing/solid–liquid reaction synthesis of bulk Cr_2AlC, Z. Metallkd. 96 (3) (2005) 291–296.
[19] C. Hu, L. He, J. Zhang, Y. Bao, J.Y. Wang, M.S. Li, Y.C. Zhou, Microstructure and properties of bulk Ta_2AlC ceramic synthesized by an in situ reaction/hot pressing method, J. Eur. Ceram. Soc. 28 (2008) 1679–1685.
[20] Z.J. Lin, M.J. Zhuo, M.S. Li, J.Y. Wang, Y.C. Zhou, Synthesis and microstructure of layered-ternary Ti_2AlN ceramic, Scripta Mater. 56 (2007) 1115–1118.
[21] D. Shan, G. Yan, L. Zhou, C. Li, J. Li, G. Liu, J. Feng, Synthesis of Ti_3SiC_2 bulks by infiltration method, J. Alloys Compd. 509 (2011) 3602–3605.
[22] C.L. Yeh, Y.G. Shen, Effects of TiC addition on formation of Ti_3SiC_2 by self-propagating high-temperature synthesis, J. Alloys Compd. 458 (2008) 286–291.
[23] C.L. Yeh, Y.G. Shen, Effects of SiC addition on formation of Ti_3SiC_2 by self-propagating high-temperature synthesis, J. Alloys Compd. 461 (2008) 654–660.
[24] C.L. Yeh, Y.G. Shen, Combustion synthesis of Ti_3AlC_2 from Ti/Al/C/TiC powder compacts, J. Alloys Compd. 466 (2008) 308–313.

[25] C.L. Yeh, Y.G. Shen, Effects of using Al_4C_3 as a reactant on formation of Ti_3AlC_2 by combustion synthesis in SHS mode, J. Alloys Compd. 473 (2009) 408–413.
[26] C.L. Yeh, C.W. Kuo, An investigation on formation of Nb_2AlC by combustion synthesis of Nb_2O_5-Al-Al_4C_3 powder compacts, J. Alloys Compd. 496 (2010) 566–571.
[27] C.L. Yeh, C.W. Kuo, Effects of Al and Al_4C_3 contents on combustion synthesis of Cr_2AlC from Cr_2O_3-Al-Al_4C_3 powder compacts, J. Alloys Compd. 509 (2011) 651–655.
[28] C.L. Yeh, C.W. Kuo, Effects of TiC addition on formation of Ti_2SnC by self-propagating combustion of Ti-Sn-C-TiC powder compacts, J. Alloys Compd. 502 (2010) 461–465.
[29] I. Salama, T. El-Raghy, M.W. Barsoum, Synthesis and mechanical properties of Nb_2AlC and $(Ti,Nb)_2AlC$, J. Alloys Compd. 347 (2002) 271–278.
[30] W.B. Tian, Z.M. Sun, H. Hashimoto, Y.L. Du, Synthesis, microstructure and properties of $(Cr_{1-x}V_x)_2AlC$ solid solutions, J. Alloys Compd. 484 (2009) 130–133.
[31] Y.C. Zhou, J.X. Chen, J.Y. Wang, Strengthening of Ti_3AlC_2 by incorporation of Si to form $Ti_3Al_{1-x}Si_xC_2$ solid solutions, Acta Mater. 54 (2006) 1317–1322.
[32] H.B. Zhang, Y.C. Zhou, Y.W. Bao, M.S. Li, J.Y. Wang, Intermediate phases in synthesis of Ti_3SiC_2 and $Ti_3Si(Al)C_2$ solid solutions from elemental powders, J. Eur. Ceram. Soc. 26 (2006) 2373–2380.
[33] D.T. Wan, Y.C. Zhou, Y.W. Bao, C.K. Yan, In situ reaction synthesis and characterization of $Ti_3Si(Al)C_2$/SiC composites, Ceram. Int. 32 (2006) 883–890.
[34] Y. Liu, J. Chen, Y. Zhou, Effect of Ti_5Si_3 on wear properties of $Ti_3Si(Al)C_2$, J. Eur. Ceram. Soc. 29 (2009) 3379–3385.
[35] M. Radovic, M.W. Barsoum, A. Ganguly, T. Zhen, P. Finkel, S.R. Kalidindi, E. Lara-Curzio, On the elastic properties and mechanical damping of Ti_3SiC_2, Ti_3GeC_2, $Ti_3Si_{0.5}Al_{0.5}C_2$ and Ti_2AlC in the 300–1573 K temperature range, Acta Mater. 54 (2006) 2757–2767.
[36] C.L. Yeh, C.W. Kuo, F.S. Wu, Effects of TiC and TiN addition on combustion synthesis of $Ti_2AlC_{0.5}N_{0.5}$ solid solutions, J. Alloys Compd. 504 (2010) 386–390.
[37] C.L. Yeh, C.W. Kuo, F.S. Wu, Formation of $Ti_2AlC_{0.5}N_{0.5}$ solid solutions by combustion synthesis of Al_4C_3-containing samples in nitrogen, J. Alloys Compd. 508 (2010) 324–328.
[38] A.G. Zhou, M.W. Barsoum, Kinking nonlinear elastic deformation of Ti_3AlC_2, Ti_2AlC, $Ti_3Al(C_{0.5}, N_{0.5})_2$ and $Ti_2Al(C_{0.5}, N_{0.5})$, J. Alloys Compd. 498 (2010) 62–70.
[39] A.G. Merzhanov, Combustion processes that synthesize materials, J. Mater. Process. Technol. 56 (1996) 222–241.
[40] Z.A. Munir, U. Anselmi-Tamburini, Self-propagating exothermic reactions: the synthesis of high-temperature materials by combustion, Mater. Sci. Rep. 3 (1989) 277–365.
[41] C.L. Yeh, Combustion synthesis: principles and applications, in: K.H.J. Buschow, R.W. Cahn, M.C. Flemings, E.J. Kramer, S. Mahajan, P. Veyssiere (Eds.), Encyclopaedia of Materials: Science and Technology, Elsevier, Amsterdam, 2010.
[42] C.L. Yeh, Y.L. Chen, An experimental study on self-propagating high-temperature synthesis in the Ta-B_4C System, J. Alloys Compd. 478 (2009) 163–167.
[43] M. Binnewies, E. Milke, Thermochemical Data of Elements and Compounds, Wiley-VCH Verlag GmbH, Weinheim/New York, 2002.